Materials Science Research International, Vol.4, No.3 pp.206-211 (1998)

General paper

EFFECT OF MICROSTRUCTURE ON CREEP AND CREEP-FATIGUE BEHAVIOR IN Ti-6Al-4V ALLOY AT ELEVATED TEMPERATURE

Seiichi NISHINO*, Kazuaki SHIOZAWA* and Yasunori AIKAWA**

*Department of Mechanical and Intellectual Systems Engineering, Toyama University, Gofuku, Toyama 930-8555, Japan

**Graduate School of Engineering, Toyama University, Gofuku, Toyama 930-8555, Japan

Abstract: The effect of microstructure on creep and creep-fatigue behavior at 773K was studied in the Ti-6Al-4V alloy having three different microstructures. The three types of microstructures prepared using different heat treatment conditions included the equiaxed α structure, lenticular α structure and bimodal (composed of equiaxed α and lenticular α) structure. Creep tests were carried out under constant load conditions at 773K in air. Creep-fatigue tests were carried out under total strain controlled conditions using a trapezoidal waveform with hold times of 2min and 10min at 773K in air. Creep rupture strength of the alloy with equiaxed α structure was similar to that of the alloy with lenticular α structure and was higher than that of the alloy with bimodal structure. The number of cycles to failure under creep-fatigue condition of the alloy with lenticular α structure was lower than that of the other two structures. The effect of microstructure on crack propagation life was small as compared with crack initiation life under creep-fatigue conditions. The fracture mode of the alloy with equiaxed α and the bimodal structures was transgranular under creep-fatigue condition. On the other hand, the crack of the alloy with lenticular α structure was initiated and propagated at the interface between the α layer precipitated at the grain boundary and the lenticular α structure.

Key words: *Creep, Low-cycle fatigue, High temperature, Heat treatments, Ti-6Al-4V alloy, Strain hold, Microstructure*

1. INTRODUCTION

Increased uses of titanium alloys in hot sections of engines, airframes and other mechanical parts have recently attracted special attention. Engineering components are usually subjected to cyclic loads due to vibration, power changes and temperature changes. It is important work to clarify the mechanical properties, such as creep strength and low-cycle fatigue strength, for using titanium alloys at elevated temperatures. The mechanical properties of the titanium alloys depend upon the microstructure[1-7]. It is very important to understand the microstructural effects of the titanium alloys on creep and low-cycle fatigue strength at elevated temperature.

It has been reported that the α+β processed titanium alloy (equiaxed α structure) has a longer low-cycle fatigue life at elevated temperature than that of the β processed titanium alloy (lenticular α structure)[1,7]. This is due to a higher resistance to crack initiation in the α+β processed titanium alloy.

In a series of studies to establish the relationship between microstructure and the mechanical properties of titanium alloys at elevated temperature, the effect of microstructure on creep and creep-fatigue behavior in Ti-6Al-4V alloy was investigated in this study. The three kinds of microstructures in the Ti-6Al-4V alloy were prepared by different heat treatments included the equiaxed α structure, lenticular α structure and bimodal structure (composed of equiaxed α and lenticular α structure). Creep tests were carried out under constant load condition at 773K. Creep-fatigue tests were carried out under total strain controlled conditions using a trapezoidal waveform with strain hold-times of 2min and 10min at 773K in air.

Received August 25, 1997

2. EXPERIMENTAL PROCEDURE

2.1. Specimen

The material used in this study was a titanium alloy, Ti-6Al-4V alloy. The chemical composition in weight percent is 6.29Al, 4.13V, 0.194Fe, 0.166O, 0.0077 N, 0.0044H, 0.0055C, <0.001Y and balance of Ti. Three kinds of microstructures were obtained by the different heat treatments; equiaxed α structure (1123K for 6h, air cooled, hereafter referred to as E), lenticular α structure (1373K for 1h, air cooled, hereafter referred to as L) and bimodal structure (1223K for 2h, air cooled, 993K for 2h, air cooled, hereafter referred to as E+L). The microstructures obtained by these heat treatments are shown in Fig.1. The equiaxed α structure has α-phase with an average grain size of 8.7μm. The lenticular α structure

has lenticular α-phase and β-phase which are parallel to each other in a colony. The grain size of prior β grain of lenticular α structure is above 1mm. The bimodal structure is made of the equiaxed α-phase with an average grain size of 9.0μm and the lenticular α-phase with an average grain size of 9.3μm. The area ratio of equiaxed α-phase and lenticular α-phase of the lenticular α structure is 0.67:0.33. Mechanical properties of the specimen at room temperature and at 773K are shown in Table 1. The elongation, δ, and reduction of area, ψ, of the alloy with lenticular α structure are lower than those of the other two structures. The tensile strength, σ_B, and proof strength, $\sigma_{0.2}$, of the three structures are almost the same.

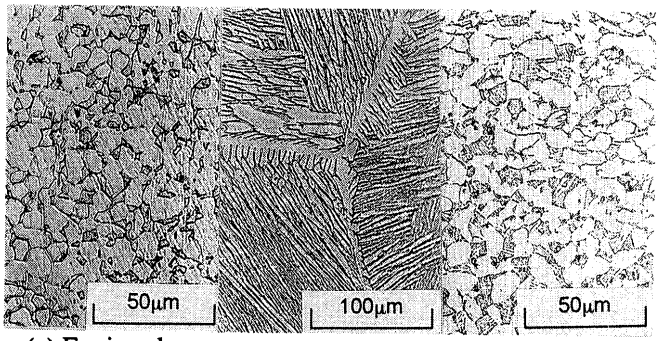

(a) Equiaxed α structure. (b) Lenticular α structure. (c) Bimodal structure.

Fig. 1. Microstructures of Ti-6Al-4V.

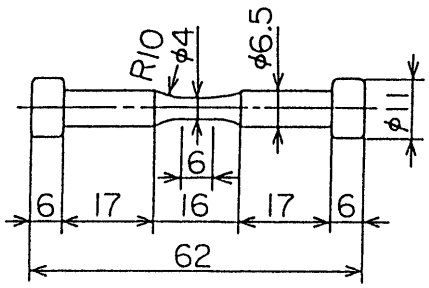

Fig. 2. Shape and dimensions of test specimen.

The shape and dimensions of the specimen used in this study are shown in Fig.2. Specimens were machined from 12mm thick rolled plates after the heat treatment mentioned above. The specimen axis agreed with the rolling direction of the plate.

2.2. Test Procedure

Creep tests were performed at 773K in air. Low-cycle fatigue tests were performed at 773K in air using a strain controlled trapezoidal waveform with strain hold times of 2min and 10min, and a loading and unloading strain rate of 0.5%/s. The number of cycles to failure was defined as the cycle at which the tensile stress amplitude decreased to 3/4 of the maximum value.

In this study, the number of cycles to crack initiation, N_i, was defined by the D.C. potential method[7]. A constant current of 20A was supplied to the specimen, and the electric potential between the gage section of the specimen which is 16mm was detected by a digital potentiometer with a resolution of 0.1μV. Stainless wires were used as sensing wires. The N_i value was defined as the number of cycles when the potential value increased to 0.2% from the initial value during the fatigue. The N_i corresponds to the cycles at the surface crack length of about 550μm [7].

3. EXPERIMENTAL RESULTS AND DISCUSSION

3.1. Creep Test

3.1.1. Creep rupture strength and deformation behavior

Figure 3 shows the creep life diagram of Ti-6Al-4V at 773K. Creep strength of the equiaxed α structure was similar to that of the lenticular α structure and was higher than that of the bimodal structure. In the triangular waveform, the highest low-cycle fatigue strength was found in the bimodal structure, followed by the equiaxed α structure, and the lowest was the lenticular α structure[7]. Thus the difference in creep strength with microstructure differed from that of low-cycle fatigue

Table 1. Mechanical properties of Ti-6Al-4V.

Microstructure	Temp. T(K)	Young's modulus E(GPa)	Proof stress $\sigma_{0.2}$(MPa)	Tensile strength σ_B(MPa)	Elongation δ(%)	Reduction of area ψ(%)	Vickers hardness Hv(200g)
Equiaxed α	R.T.	93.2	827	905	13.5	27.7	325
structure	773	66.6	470	569	28.2	53.8	—
Lenticular α	R.T.	87.8	831	923	3.7	14.2	334
structure	773	72.5	459	583	27.2	49.6	—
Bimodal	R.T.	90.7	869	934	12.8	28.2	335
structure	773	67.9	454	573	24.7	41.6	—

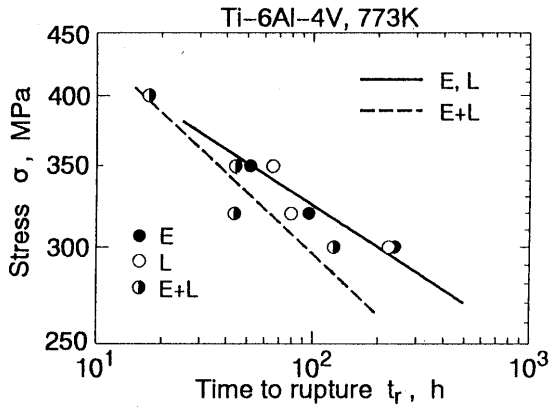

Fig. 3. Creep life diagram of Ti-6Al-4V at 773K.

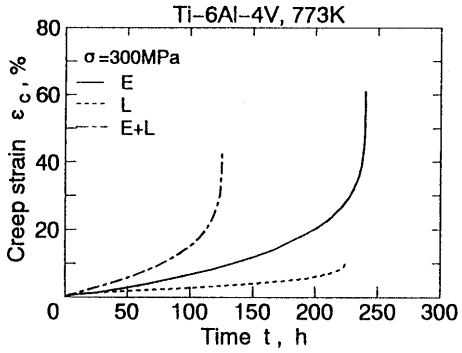

Fig. 4. Typical example of creep curves of Ti-6Al-4V at 773K (σ=300MPa).

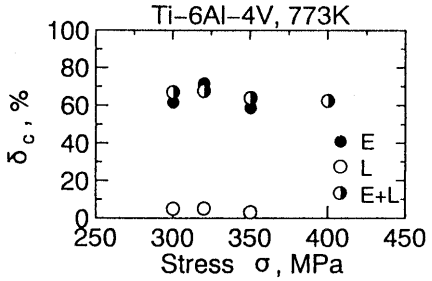

Fig. 5. Relationship between elongation, δ_c, and applied stress in creep tests.

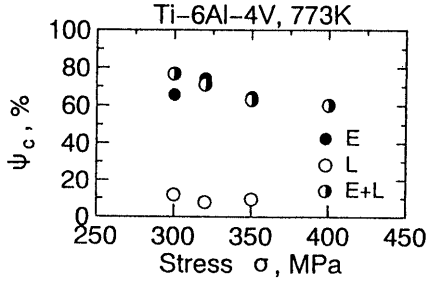

Fig. 6. Relationship between reduction of area, ψ_c, and applied stress in creep tests.

strength.

Figure 4 shows a typical example of creep curves obtained in the creep tests. Creep strain of the bimodal structure is the highest, followed by the equiaxed α structure, and that of the alloy with lenticular α structure is the lowest. Creep elongation and reduction of area of the lenticular α structure are much smaller than those of the other two structures, as shown in Fig.5 and Fig.6, respectively.

Figure 7 shows a typical example of creep strain rate with time at σ=300MPa. The minimum creep strain rate of the equiaxed α and the bimodal structures occurred during the early stage of the creep process. On the other hand, the creep strain rate of the lenticular α structure has a constant value in the period between $0.15t_r$ to $0.75t_r$, where t_r is the rupture time of the specimen. The minimum creep strain rate of the bimodal structure is the highest, followed by the equiaxed α structure, while the lenticular α structure is the lowest.

Figure 8 shows the relationship between minimum creep rate and applied stress. Linear relationship is found as Norton's law applies. The slope of the lines in this figure, i.e., the exponent of Norton's law, has the

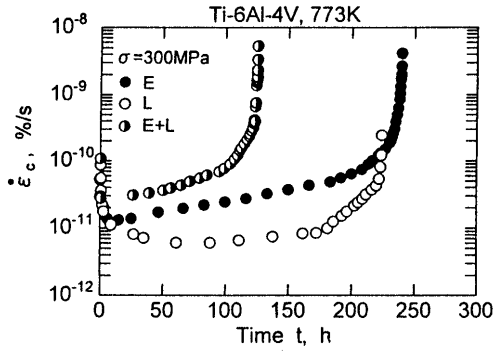

Fig. 7. Variation of creep strain rate with time at σ=300MPa.

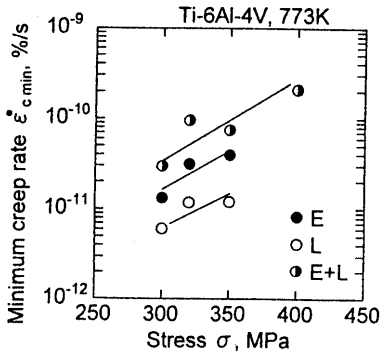

Fig. 8. Relationship between minimum creep rate, $\dot{\varepsilon}_{c\,min}$, and applied stress.

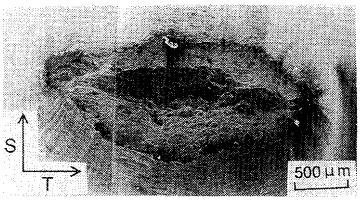

(a) Equiaxed α structure.

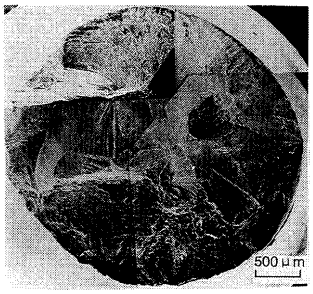

(b) Lenticular α structure.

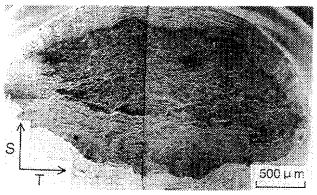

(c) Bimodal structure.

Fig. 9. Macroscopic observation of fracture surface after creep test at σ=300MPa.

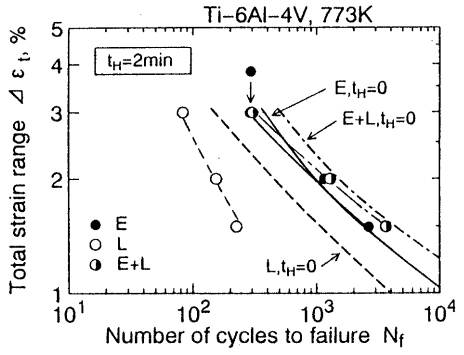

(a) t_H=2min

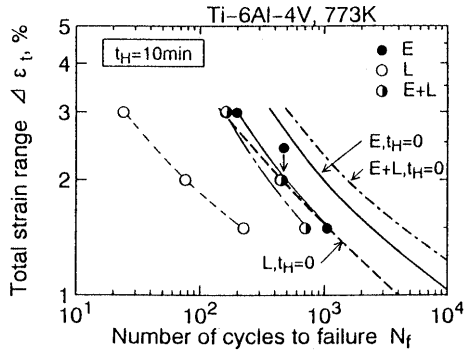

(b) t_H=10min

Fig. 10. Relationship between total strain range, $\Delta\varepsilon_t$, and number of cycles to failure, N_f.

same value for these microstructures.

3.1.2. Fractography of creep fracture surface

Figure 9 shows the macroscopic fracture surface after the creep test. In this figure, S is the thickness direction of the rolled plate and T is the transverse direction to the rolling direction of the plate. For the equiaxed α and the bimodal structures, the diameter of the specimen was reduced in the S direction, and exhibited transgranular fracture. This is because the grain of the equiaxed α and bimodal structures was elongated in the hot rolling direction. On the other hand, the area reduction of the lenticular α structure was quite small, Fig.9(b), and it corresponds with intergranular fracture. The reason why the creep ductility of the lenticular α structure is lower than that of the other two structures is that intergranular fracture occurs in the lenticular α structure.

3.2. Low-Cycle Fatigue Test

3.2.1. Low-cycle fatigue life

Figure 10 shows the relationship between the total strain range and the number of cycles to failure in the low-cycle fatigue tests using a trapezoidal waveform. Low-cycle fatigue life using a triangular waveform is superimposed in the figure as t_H=0[7]. Fatigue life using the trapezoidal waveform is lower than that using the triangular waveform for all the structures. In the case of t_H=2min, the highest low-cycle fatigue strength was found in the bimodal structure, followed by the equiaxed α structure, and the lowest was the lenticular α structure, of which the trend is similar to that of t_H=0. However, in the case of t_H=10min, fatigue life of the equiaxed α structure is higher than that of the bimodal structure.

3.2.2. Crack initiation and propagation behavior

The experimental relationship of the t_H=10min test between total strain range, $\Delta\varepsilon_t$, the number of cycles to crack initiation, N_i, and the number of cycles for crack propagation, N_p, is shown in Fig.11, which were obtained using the D.C. potential method. The test results for the triangular wave, t_H=0, are also included in this figure for comparing the results of the trapezoidal wave[7]. It can be seen from this figure that crack initiation life in the trapezoidal waveform decreased as compared with that of triangular waveform for each structure.

The number of cycles for crack propagation of the equiaxed α structure was similar to that of the bimodal

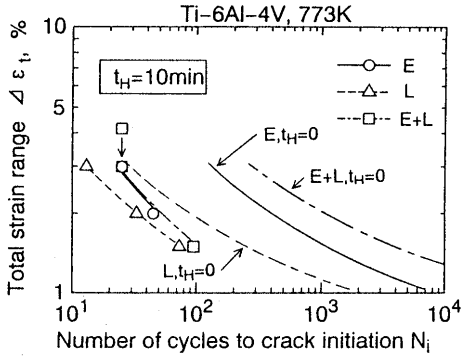

(a) N_i

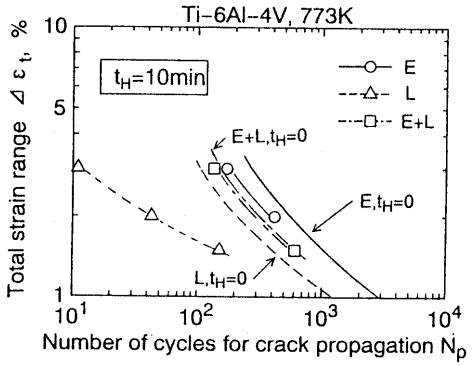

(b) N_p

Fig.11. Relationship between total strain range, $\Delta\varepsilon_t$, and number of cycles to crack initiation, N_i, and number of cycles for crack propagation, N_p (t_H=10min).

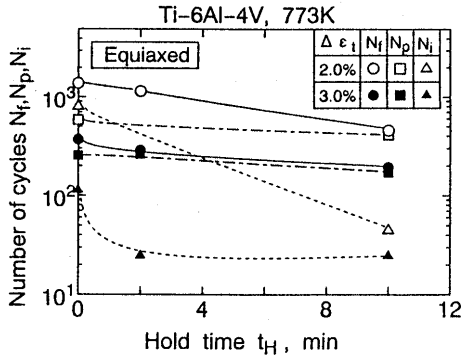

(a) Equiaxed α structure.

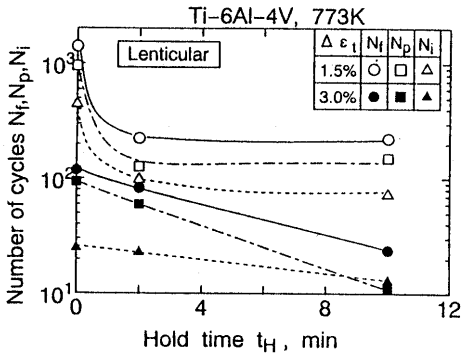

(b) Lenticular α structure.

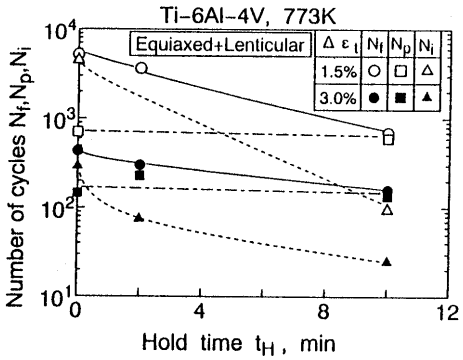

(c) Bimodal structure.

Fig. 12. Relationship between N_i, N_p, N_f and hold time t_H.

structure, while that of the lenticular α structure was inferior to that of the other two structures. The number of cycles for crack propagation of the lenticular α structure significantly decreased by introducing a hold time as compared with that of the other two structures.

In order to discuss the effect of hold time on fatigue behavior, Fig.12 shows the relationship between the number of cycles to crack initiation, N_i, the number of cycles for crack propagation, N_p, the number of cycles to failure, N_f, and hold time. For the equiaxed α and the bimodal structures, the value of N_i decreased with increasing hold time, though the value of N_p did not change with hold time. The variation in crack initiation life, N_i, of the equiaxed α and the bimodal structures with hold time corresponds with that of fatigue life, N_f. The effect of strain hold time on low-cycle fatigue life of both materials will only appear as an acceleration of crack initiation and small crack growth. On the other hand, both N_i and N_p values of the lenticular α structure decreased with increasing hold time. It is concluded based on this experimental evidence that the effect of strain hold time on fatigue behavior is different based on the microstructure of the specimens.

3.2.3. Crack observation after low-cycle fatigue test

Figure 13 shows typical observations of cracks on the specimen surface after low-cycle fatigue test under trapezoidal waveform. For the equiaxed α and the bimodal structures shown in Figs.13(a) and (c), a crack initiated in the equiaxed α–phase, and propagated perpendicular

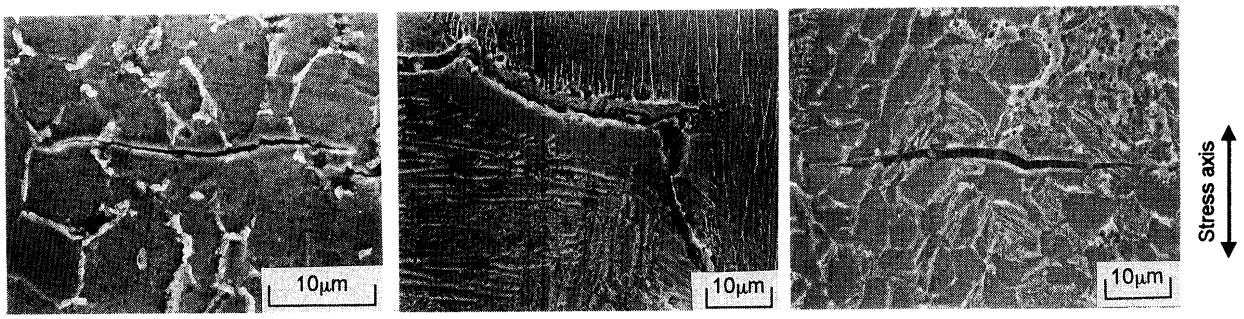

(a) Equiaxed a structure. (b) Lenticular a structure. (c) Bimodal structure.

Fig. 13. Typical micrographs of crack on the specimen surface after low-cycle fatigue test under trapezoidal waveform (t_H=10min, $\Delta\varepsilon_t$=1.5%).

to the stress axis. For the lenticular α structure in Fig.13(b), a crack was initiated and propagated along the interface between the α layer precipitated at the grain boundary and the lenticular α-phase in the grain. As a results, the fracture surface revealed intergranular fracture mode. It was reported previously that, for the equiaxed α and the bimodal structures, the crack initiated at the specimen surface due to crystal slip and transgranularly propagated under low-cycle fatigue with no strain hold time[7]. This is the same trend as observed in this work. It was reported that for the lenticular α structure, the intergranular cracking was observed at the crack initiation site in the early crack growth region, and the fracture mode changed to transgranular cracking under low-cycle fatigue with the triangular waveform[7]. This is different from the observations in this work. The reason why the effect of hold time on crack propagation cycles of the lenticular α structure was different from that of the other two structures was that the fracture mode of the lenticular α structure changed from transgranular cracking to intergranular cracking due to the creep damage during strain hold.

4. CONCLUSIONS

(1) Creep rupture strength of the alloy with equiaxed α structure was similar to that of the alloy with lenticular α structure and was higher than that of the alloy with bimodal structure.

(2) The number of cycles to failure of the alloy with lenticular α structure was lower than that of the other two structures under creep-fatigue conditions.

(3) The effect of microstructure on crack propagation life was low in comparison with the crack initiation life under creep-fatigue conditions in the equiaxed α and the bimodal structures. On the other hand, the number of cycles to crack initiation and that for propagation of the lenticular α structure decreased with increasing hold time.

(4) Transgranular fracture occurred in the equiaxed α and bimodal structures under creep-fatigue conditions. On the other hand, cracking of the lenticular α structure was initiated and propagated at the interface between the α layer precipitated at grain boundaries and lenticular α-phase.

REFERENCES

1. D. Eylon, J.A. Hall, C.M. Pierce and D.L. Ruckle, Metall. Trans. A, **7A** (1976) 1817.
2. D. Eylon, S. Fujishiro, P.J. Postans and F.H. Froes, J. Metals, **36** (1984) 55.
3. C. Hoffman, D. Eylon and A.J. McEvily, ASTM STP 770 (1982) 5.
4. K. Minagawa, Iron and Steel, **75** (1989) 36.
5. O. Izumi, Iron and Steel, **73** (1987) 411.
6. P.S. Webster and A.C. Pickard, J. Strain Analysis, **22** (1987) 145.
7. K. Shiozawa, S. Nishino and Y. Aikawa, J. Soc. Mater. Sci., Japan, **44** (1995) 1372.